ISSN 0030-400X, Optics and Spectroscopy, 2018, Vol. 125, No. 1, pp. 14–21. © Pleiades Publishing, Ltd., 2018.

SPECTROSCOPY AND PHYSICS OF ATOMS AND MOLECULES

Structural, Spectroscopic, Antimicrobial Activity and DFT Studies on 4-Methyl-*N*-(4-methylphenylsulfonyl)-*N*-phenylbenzenesulfonamide[1]

Bilge Eren[a], Fadime Özdemir Koçak[b], and Namık Özdemir[c, *]

[a] *Department of Chemistry, Faculty of Arts and Sciences, Bilecik Şeyh Edebali University, Bilecik, 11210 Turkey*

[b] *Department of Nursing, School of Health, Bilecik Şeyh Edebali University, Bilecik, 11210 Turkey*

[c] *Department of Mathematics and Science Education, Faculty of Education, Ondokuz Mayıs University, Samsun, 55139 Turkey*

**e-mail: namiko@omu.edu.tr*

Received October 1, 2017

Abstract—This study reports the structural characterization of a disulfonimide derivative, 4-methyl-*N*-(4-methylphenylsulfonyl)-*N*-phenylbenzenesulfonamide (MPBSA), using spectroscopic and quantum chemical methods. The molecule was characterized with FT-IR, ^{1}H ^{13}C NMR and UV-Vis spectroscopies. Quantum chemical calculations of molecular geometry, vibrational wavenumbers and gauge including atomic orbital (GIAO) ^{1}H and ^{13}C-NMR chemical shifts of the compound were carried out by using density functional method (DFT) at B3LYP/6–311++G(d,p) level of theory. Electronic absorption spectra of the compound have been computed using the time-dependent density functional theory (TD-DFT) method at the same level. A satisfactory consistency between the experimental and theoretical findings was obtained. The antimicrobial activity screening of the compound was performed on some bacteria and fungus species using microdilution method. The results showed that the title molecule have noteworthy antibacterial and antifungal activities.

DOI: 10.1134/S0030400X18070068

INTRODUCTION

Sulfonamides have called as sulfa drugs since the invention of the first member prontosil, as the first antimicrobial agent [1]. They are an important class of compound in the field of chemistry and medicine since many years. Several derivatives of them used as chemotherapeutic agent for their antibacterial [2, 3], antifungal [4], antitumor [5], hypoglycemic [6] effects. The title compound structurally belongs to the disulfonimide group. Disulfonimides have two sulfone group connected to the nitrogen atom in their structure. They are also sulfonamide derivatives and commonly used in medicine for their antitumor effects and CA inhibitory properties [7, 8].

The density functional theory (DFT) methods have been recently used to analyze the structures, dipole moments, vibrational frequencies, nuclear magnetic resonance (NMR) chemical shifts, optical properties, molecular electrostatic potentials of organic compounds with high degree of accuracy in comparison to those of experimental values [9–13]. In our previous work, we have reported the synthesis and single crystal X-ray diffraction characterization of 4-methyl-*N*-(4-methylphenylsulfonyl)-*N*-phenylbenzenesulfonamide (MPBSA) [14]. In the present work, MPBSA was further investigated by FT-IR, ^{1}H and ^{13}C NMR and UV-Vis spectroscopies. The antibacterial activity of the MPBSA were also studied against some bacteria and fungus species. Additionally, detailed theoretical analysis at the B3LYP/6–311++G(d,p) level of theory was performed and compared with experimental findings.

To the best of our knowledge, neither detailed spectroscopic investigation nor the theoretical studies on the title compound have been reported yet. The knowledge of physicochemical properties, structural parameters and spectroscopic features about this bioactive molecule will provide a deeper comprehension on its chemical and biological behavior.

MATERIALS AND METHODS

Instrumentation

The ATR-IR spectrum of MPBSA was recorded in the range of 4000–650 cm^{-1} with a Spectrum-100 Frontier spectrometer. The ^{1}H and ^{13}C-NMR spectra were recorded on a Varian Mercury 500 MHz NMR

[1] The article is published in the original.

spectrometer using tetramethylsilane (TMS) as an internal standard and DMSO-d_6 as solvent. Chemical shifts are given in parts per million with reference to TMS. The UV-Vis spectra were measured on a Unicam-2 UV-Vis spectrometer in DMSO.

Computational Procedure

The DFT calculations with the three-parameter hybrid density functional (B3LYP) [15, 16] and B3LYP/6−311++G(d,p) basis set [17] were performed using the Gaussian 03 software package [18] and GaussView visualization program [19]. The calculated vibrational frequencies ascertained that the structure was stable (no imaginary frequencies). A scale factor of 0.9679 [20] has been used to correct the calculated harmonic vibrational frequencies. The ^{1}H and ^{13}C NMR chemical shifts were obtained via the gauge-independent atomic orbital (GIAO) approach [21, 22] at the same level, in which solvent effects were included using the default method [23], while the electronic absorption spectra were obtained using the time dependent density functional theory (TD-DFT) [24, 25].

Microbial Strains and Assays for in Vitro Antimicrobial Activity

Antimicrobial activities were determined by using culture of *Bacillus cereus* ATCC 7064, *Staphylococcus aureus* ATCC 25923 as Gram positive bacteria and *Escherichia coli* ATCC 25922, *Pseudomonas aeruginosa* ATCC 27853 as Gram negative bacteria and *Aspergillus parasiticus* NRRL 1957, *Candida albicans* ATCC 10231 as fungus.

The minimal inhibitory concentrations (MICs) of MPBSA were tested against bacteria and fungus were determined by using a broth microdilution method in 96 multi-well microtitre plates [26, 27]. After 24 or 48 h cultivation, microbial suspensions were made in Mueller Hinton broth and their turbidity was standardized to 0.5 McFarland. Dimethyl sulphoxide was used to dissolve and to dilute sample. A serial double dilution of the sample was prepared in 96 well microtitre plates, using method of Sarker et al. [28]. The stock concentration was 10 mg/mL. The lowest concentration of the sample that inhibited visible growth was taken as the MIC value. To determine minimal bactericidal concentration (MBC), broth was taken from each well without visible growth and inoculated in Mueller Hinton agar for 24–48 h at 37°C. The lowest concentration of the tested sample that killed 99.9% of bacterial cells was evaluated as the MBC value. Tests were carried out in triplicate.

Table 1. Selected experimental and optimized geometric parameters for MPBSA

Parameters	X-ray	DFT
Bond lengths, Å		
S1–O1	1.4224(12)	1.457
S1–O2	1.4203(13)	1.456
S1–N1	1.6822(9)	1.739
S1–C1	1.7547(17)	1.792
N1–C7	1.447(3)	1.439
Bond angles, deg		
O2–S1–O1	119.75(8)	121.26
O2–S1–N1	107.78(8)	106.94
O1–S1–N1	105.59(7)	104.79
O2–S1–C1	109.53(8)	109.28
O1–S1–C1	108.00(8)	107.87
N1–S1–C1	105.22(5)	105.60
S1–N1–S1^{i}	124.84(11)	122.05
C7–N1–S1	117.58(5)	118.98

Symmetry code: ^{i} $-x+1, y, -z+3/2$.

RESULTS AND DISCUSSION

Theoretical Structure

The X-ray structure of the compound, which has been reported previously (Fig. 1a) [14], was optimized by DFT method with the 6–311++G(d,p) basis set in the gas phase. Some of the optimized parameters (bond lengths, bond angles, and dihedral angles) of the compound are listed in Table 1 along with the corresponding experimental parameters.

It is seen from Table 1 that the theoretical geometric parameters are in good agreement with the experimental ones. The maximum deviation of the bond lengths is 0.057 Å at S1–N1 and the greatest deviation of the bond angles is 2.79° at S1–N1–S1^{i}. In the X-ray structure, the two methylphenyl rings are inclined at an angle of 87.79(9)°, while the benzene ring makes a dihedral angle of 51.48(15)° with the planes of the two methylphenyl rings. In the optimized structure these dihedral angles are found to be 64.79° and 42.26°, respectively. When the experimental and computed structures are globally compared by overlaying them using PLATON [29], the determined bond and angle fit values are 0.026 Å and 0.763° (Fig. 1b). Consequently, the theoretical structure sufficiently resembles to the X-ray ones, and the level of theory can be used to examine the other properties.

IR Spectroscopy

FT-IR spectrum of the MPBSA along with the calculated one is given in Fig. 2. The vibrational bands assignments have been done by using Gauss View

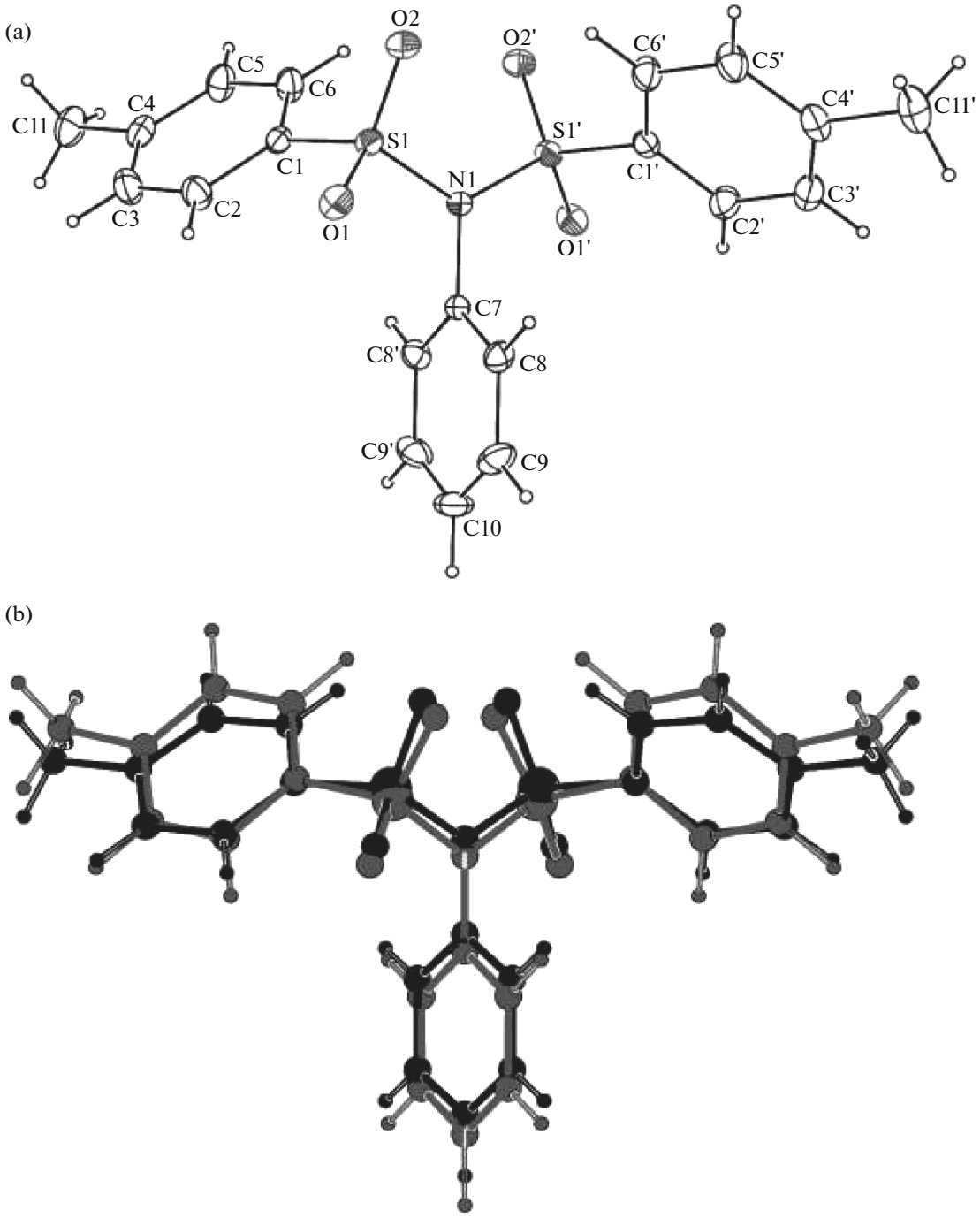

Fig. 1. (a) Experimental structure of MPBSA with the atom-numbering scheme [14]. (b) A molecular fit of the experimental and calculated structures shown in black and white, respectively.

molecular visualization program. The aromatic structure shows a couple of C–H stretching modes (3057, 3070, 3094 cm^{-1}) in the region 3100–3000 cm^{-1} which is the characteristic region for the ready identification of C–H stretching vibrations [30, 31]. These bands have been calculated at 3066, 3086 and 3118 cm^{-1}, respectively. The aromatic C–H in-plane bending modes of benzene and its derivatives are observed as weak intensity peaks in the region 1300–1000 cm^{-1} in the vibrational spectra, while the C–H out-of-plane bending vibrations occur in the range 1000–750 cm^{-1} in the aromatic compounds [13, 32, 33]. The weak bands observed at 753 and 839 cm^{-1} are assigned to C–H out-of-plane bending modes that have been calculated at 786 and 823 cm^{-1}, respectively. Also, the

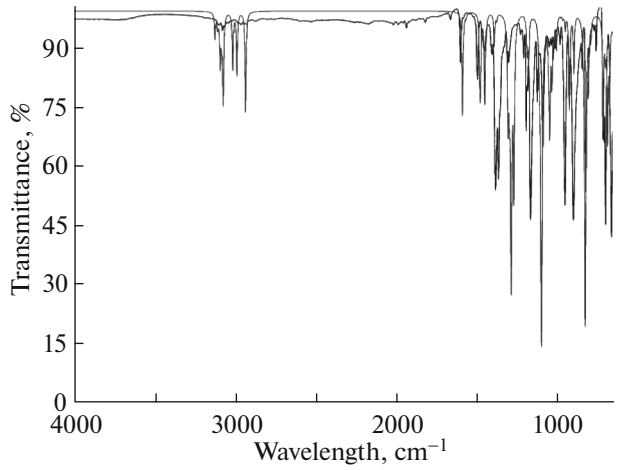

Fig. 2. The experimentally recorded and theoretically simulated FT-IR spectra of MPBSA.

bands observed at 1018 and 1043 cm^{-1} are assigned to aryl C–H in-plane bending vibrations, which are in coincidence with theoretical values of 1014 and 1065 cm^{-1}. In general, the calculated aromatic C–H vibrations (stretching, in-plane and out-of-plane bending) are in good agreement with experimentally expected values given in literature [30–35]. The C–H asymmetric and symmetric stretching vibrations of the CH_3 group are seen at 2959 and 2926 cm^{-1} as expected. These bands appeared at 2982 and 2928 cm^{-1} in the theoretical spectra, respectively.

When evaluated in terms of $S{=}O_2$ vibrations, the asymmetric and symmetric $S{=}O_2$ stretching vibrations appear in the range 1330 ± 30 cm^{-1} and 1160 ± 30 cm^{-1}, respectively, both with strong intensity [36, 37]. For MPBSA molecule, the asymmetric stretching mode was recorded at 1370 cm^{-1}, while the symmetric mode was obtained at 1160 cm^{-1}. We calculated the asymmetric and symmetric $S{=}O_2$ stretching vibrations at 1279 and 1092 cm^{-1}, respectively.

The aromatic C=C stretching vibrations generally occur in the region of 1625–1430 cm^{-1}. The bands are variable in intensity and observed at 1625–1590, 1590–1575, 1540–1470, 1460–1430 and 1380–1280 cm^{-1} wavenumber ranges for the five bands in the region [13, 33]. The medium bands observed at 1595 and 1294 cm^{-1} were assigned to aromatic C=C stretching vibrations that have been calculated at 1582 and 1289 cm^{-1}, respectively.

The assignments of the C–N stretching wavenumbers were made from analogy with the similar molecules in the literature [13, 33, 38]. The strong peak at 1085 cm^{-1} is attributed to the fundamental C–N stretching vibration, which was observed at 1181 cm^{-1} in the theoretical spectrum. The S–N stretching vibration exhibits a medium band in the range 905 ± 70 cm^{-1} [36]. The infrared studies of some arylsulfonamide [39] and N-aryl-methanesulfonamide derivatives [40] are also assigned in the region 924–906 and 926–833 cm^{-1}. The bands at 919 and 892 cm^{-1} are assigned to S–N stretching vibration that have been calculated at 891 and 820 cm^{-1}, respectively.

NMR Spectroscopy

The ^{1}H and ^{13}C NMR spectra of the compound are shown in Fig. 3. The experimental ^{1}H and ^{13}C NMR chemical shifts (ppm) together with the calculated data are listed in Table 2. Since experimental ^{1}H chemical shift values were not available for individual hydrogen atoms of CH_2 group, the average of the calculated values has been given.

Table 2. Experimental and theoretical ^{13}C and ^{1}H NMR chemical shifts δ (ppm) for MPBSA

Atom	Experimental	Calculated	Atom	Experimental	Calculated
C1/C1^{i}	134.07	149.52	C11/C11^{i}	21.61	24.07
C2/C2^{i}	128.46	133.74	H2/H2^{i}	7.65 (dd)	7.47
C3/C3^{i}	130.39	136.12	H3/H3^{i}	7.47 (dd)	7.65
C4/C4^{i}	136.13	156.05	H5/H5^{i}	7.47 (dd)	7.89
C5/C5^{i}	130.39	137.28	H6/H6^{i}	7.65 (dd)	8.78
C6/C6^{i}	128.46	135.11	H8/H8^{i}	6.95–6.98 (m)	7.25
C7	145.92	140.71	H9/H9^{i}	7.45–7.41 (m)	7.70
C8/C8^{i}	129.94	142.36	H10	6.95–6.98 (m)	7.84
C9/C9^{i}	131.67	135.89	H11/H11^{i}	2.49 (s)/2.42 (s)	2.55[a]
C10	130.88	138.70			

Symmetry code: ^{i} $-x + 1, y, -z + 3/2$.
[a]Average. The atom numbering according to Fig. 1a used in the assignment of chemical shifts.

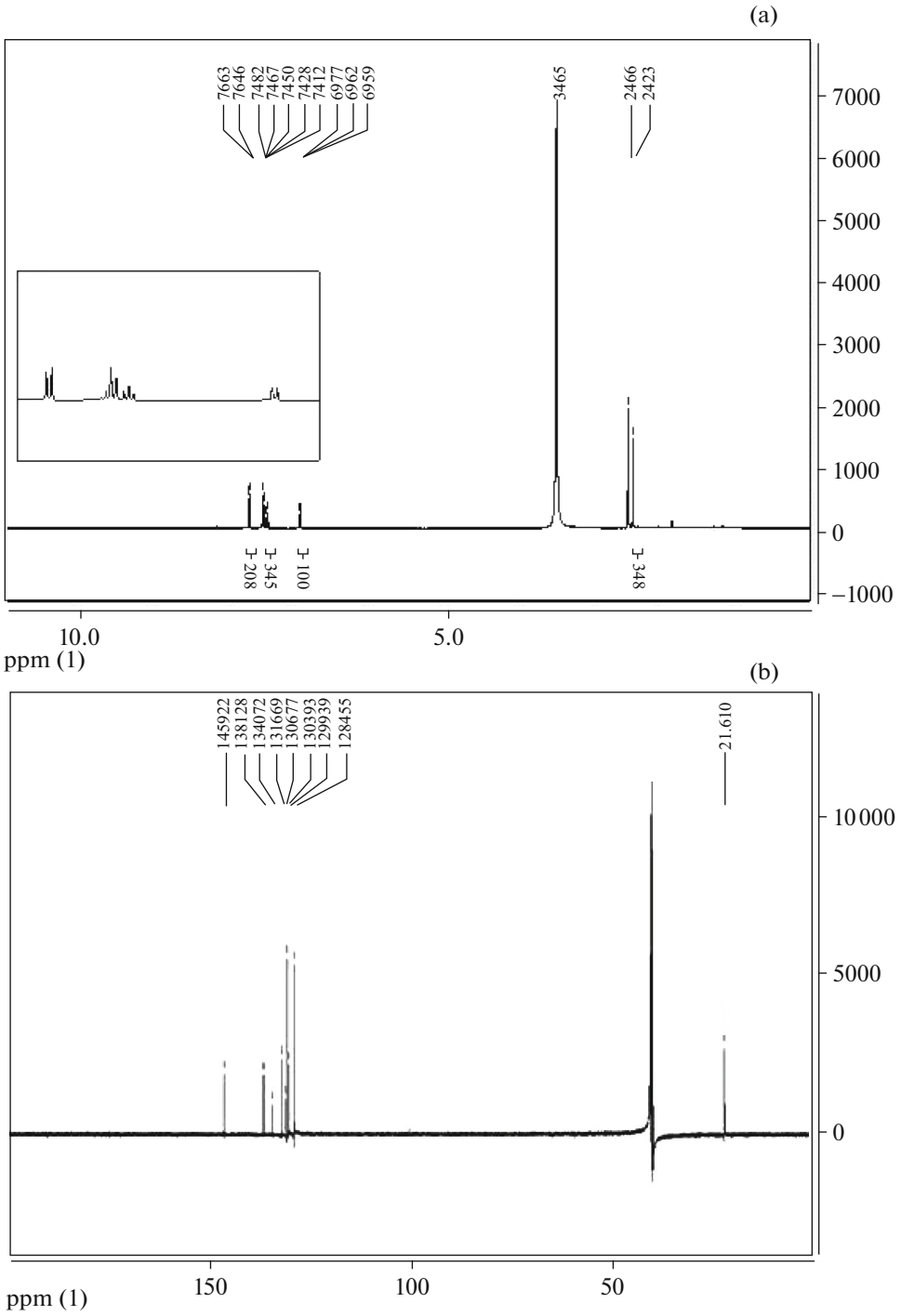

Fig. 3. (a) ^{1}H NMR spectrum of MPBSA. (b) ^{13}C NMR spectrum of MPBSA.

As shown in the ^{1}H NMR spectrum, the title molecule has five different signal groups. The singlet signals at the highest field (2.49 and 2.42 ppm) were easily assigned to methyl protons on the para positions of the phenyl rings, which has been calculated at 2.55 ppm. Aromatic protons of the benzene rings were appeared as four different signal groups in the region of 6.9–7.6 ppm. The peaks at 7.65 and 7.47 ppm are assigned to the aromatic hydrogens of the methylphenyl rings, considering the resonance and inductive effects that determines the orientation of the methyl and the sulfonyl groups. These signals were theoretically observed in the range of 7.47–8.78 ppm. The assignment of the benzene ring protons was performed

parallel to similar molecules like benzenesulfonanilide [41] or aniline [42–44] derivatives etc. The protons at the meta positions must be resonated at the down field 7.45–7.41 ppm as a result of being deshielded more than the other positions while the other protons at ortho and para positions were resonated at 6.95–6.98 ppm as expected. These signals were theoretically found at 7.70 and 7.84 ppm, respectively.

The assignments of the ^{13}C NMR signals of the benzene ring were done from analogy with similar molecules from the literature [42–44]. The carbon peak at 21.61 ppm absolutely belongs to methyl group as the only aliphatic carbon atom in the structure that has been calculated at 24.07 ppm. The medium signal at the least down field 145.92 ppm was assigned to quaternary C7 carbon which was directly connected to the electronegative nitrogen atom. This signal was monitored at 140.71 ppm in the theoretical spectrum. The other quaternary carbon in the molecule could be easily picked out from the others and assigned to the weak peak at 134.07 ppm, which was calculated at 149.52 ppm. The strong peaks at 130.39 and 128.46 ppm were normally assigned to the carbons at the 4-methylphenylsulfonyl moieties. These signals were observed computationally at 136.12 and 133.74 ppm, respectively. As shown in Table 2, all the other carbons of the title molecule appear at the expected regions and in accordance with the calculated data. As a result, the experimental ^{1}H and ^{13}C spectra data are compatible with the structure and the previously reported values [42–44].

Electronic Absorption Spectroscopy

The electronic absorption spectrum of the molecule is shown in Fig. 4. The molecule has aryl rings as fundamental chromophore in the UV-Vis region. When we consider the simplest aromatic compound benzene, it shows a primary band at 204 nm ($\varepsilon = 8000$) and a secondary fine structure band at 256 nm ($\varepsilon = 200$). Both of them are based on $\pi \rightarrow \pi^*$ transitions [45, 46]. Substituents on the benzene ring also cause bathochromic and hypsochromic shifts of these peaks. Increase in the conjugation of the benzene ring also shifts these bands to longer wavelengths and cause bathochromic shift. The molecule also has a sulfone SO_2 chromophore conjugated to the benzene ring. Isolated sulfone has absorption band at <180 nm. As expected, three aryl rings and conjugation of them by the $-SO_2N-$ bridges in MPBSA molecule extend the conjugation and cause bathochromic shift on the benzene bands. As a result, MPBSA molecule shows primary band at 264 and secondary band at 276 nm based on $\pi \rightarrow \pi^*$ transitions. These values are compatible with the literature studies for some aryldisulfonamides [3].

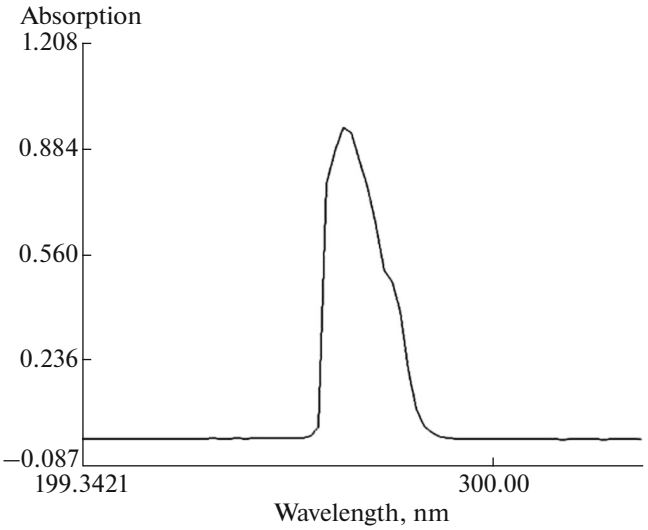

Fig. 4. UV-Vis spectrum of MPBSA in DMSO (0.26×10^{-3} M).

Electronic absorption spectrum of MPBSA was computed by the TD-DFT method at the same level. The calculated results are tabulated in Table 3. To designate the major contributions of the transitions, GaussSum program [47] was used. According to the TD-DFT calculation, two absorptions were predicted at 257 nm with a major transition contribution from HOMO to LUMO (95%) and at 250 nm with a major transition contribution from HOMO to LUMO+1 (72%). The selected frontier molecular orbitals of MPBSA are given in Fig. 5. The HOMO–LUMO gap (ΔE) is an indicator of the chemical reactivity and chemical hardness–softness of a molecule, being small for soft molecules and being large for hard molecules. According to the computed gap value of 5.45 eV, the title molecule can be accepted as a hard molecule.

Table 3. Experimental and theoretical electronic absorption spectra values of MPBSA

Experimental			Theoretical		
λ_{max}, nm	Abs.	ε	λ_{max}, nm	Oscillator strengths	Transitions
276	0.476	1725	257	0.379	HOMO → LUMO (95%)
264	0.948	3550	250	0.112	HOMO → LUMO+1 (72%)

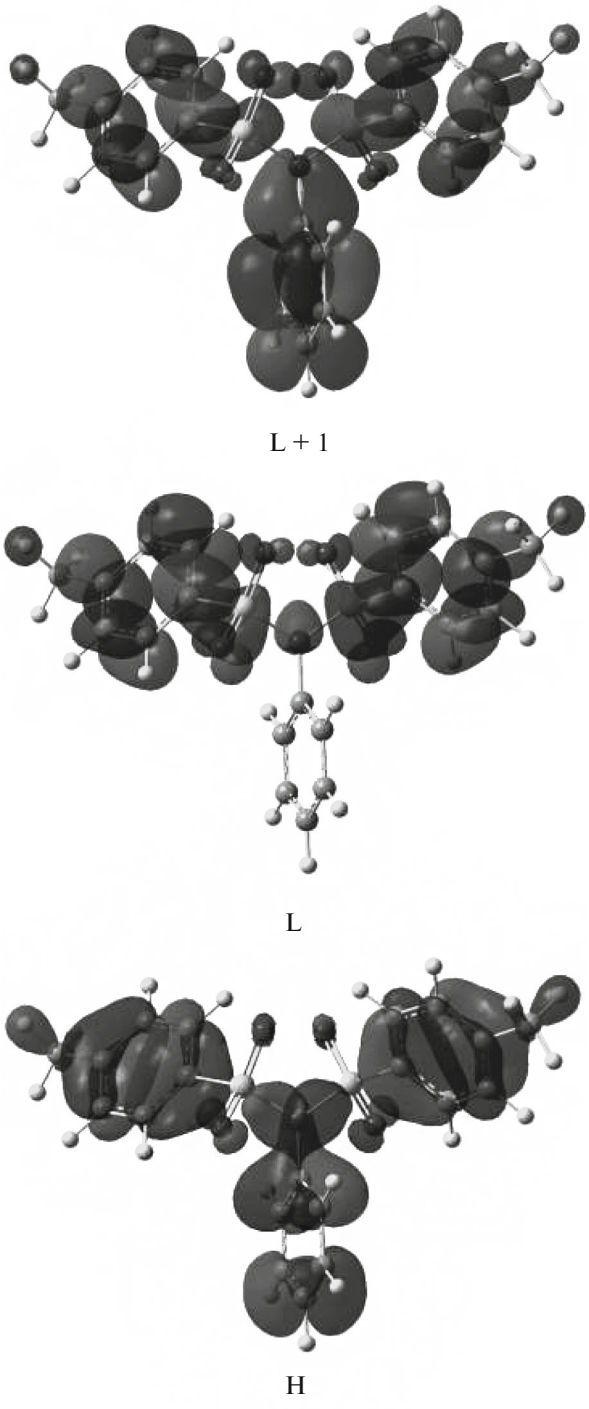

Fig. 5. Selected molecular orbital surfaces of MPBSA (H: HOMO, L: LUMO).

Antimicrobial Activity

Antimicrobial activity of MPBSA was carried out using culture of *B. cereus*, *S. aureus* as gram-positive bacteria and *E. coli*, *P. aeruginosa* as gram-negative bacteria and *A. parasiticus*, *C. albicans* as fungus. The MIC determinations were obtained by broth microdilution assay. The minimal bactericidal concentration (MBC) values of MPBSA on aforementioned species was determined between the dose of 500–2000 μg/mL. Antimicrobial activity results of MPBSA in terms of MIC values are listed in Table 4. The MIC values of MPBSA was determined between the dose of 62.5–1000 μg/mL against aforementioned Gram-positive, Gram-negative bacteria and fungus species. The results clearly indicated that the compound has the capacity of inhibiting the metabolic growth of some microorganisms investigated. The compound showed remarkable antimicrobial activity against *B. cereus* (MIC = 125 μg/mL) and antifungal activity against *C. albicans* (MIC = 62.5 μg/mL). This value is also at a level that can be considered well. It can be thought that the remarkable activity of this compound may be arising from the sulfonamide group ($-SO_2N-$), which may play an important role in the antibacterial activity [1–4].

Table 4. Antimicrobial activity of MPBSA in terms of minimal inhibitory concentrations (MICs)

Microorganism	MIC (μg/mL)
C. albicans	62.5
A. parasiticus	1000
E. coli	500
P. aeroginosa	250
B. cereus	125
S. aureus	500

CONCLUSIONS

In this work, a disulfonimide derivative was characterized by FT-IR, ^1H and ^{13}C NMR and UV-Vis spectroscopies. The structural and spectral properties obtained experimentally were also studied by some quantum mechanics calculations at the B3LYP/6–311++G(d,p) level. TD-DFT calculations were also performed to determine possible electronic transitions. The FT-IR and NMR spectra clearly confirm the molecular structure. Inspite of the little differences, an acceptable correlation between the computational and experimental results was found. The antimicrobial activity screening of the molecule was carried out on some bacteria and fungus species via microdilution method. The findings showed that the molecule have remarkable antibacterial and antifungal activities.

ACKNOWLEDGMENTS

This study was supported financially by Bilecik Şeyh Edebali University (project no. 2011-02-BİL.04-03).

REFERENCES

1. J. E. Lesch, *The First Miracle Drugs: How the Sulfa Drugs Transformed Medicine* (Oxford Univ. Press, New York, 2007).
2. K. Isik and F. Özdemir-Kocak, Microbiol. Res. **164**, 49 (2009).
3. S. Alyar, H. Zengin, N. Ozbek, and N. Karacan, J. Mol. Struct. **992**, 27 (2011).
4. Z. H. Chohan, M. H. Youssoufi, A. Jarrahpour, and T. B. Hadda, Eur. J. Med. Chem. **45**, 1189 (2010).
5. N. S. El-Sayed, E. R. El-Bendary, S. M. El-Ashry, and M. M. El-Kerdawy, Eur. J. Med. Chem. **46**, 3714 (2011).
6. K. Seri, K. Sanai, K. Kurashima, Y. Imamura, and H. Akita, Eur. J. Pharm. **389**, 253 (2000).
7. C. T. Supuran, F. Briganti, S. Tilli, W. R. Chegwidden, and A. Scozzafava, Bioorg. Med. Chem. **9**, 703 (2000).
8. P. A. Boriack-Sjodin, S. Zeitlin, D. W. Christianson, H.-H. Chen, L. Crenshaw, S. Gross, A. Dantanarayana, P. Delgado, J. A. May, and T. Dean, Protein Sci. **7**, 2483 (1998).
9. H. Tanak, A. Ağar, and M. Yavuz, J. Mol. Model. **16**, 577 (2010).
10. A. Ünal, M. Şenyel, and Ş. Şentürk, Vibrat. Spectrosc. **50**, 277 (2009).
11. N. Özdemir, B. Eren, M. Dinçer, and Y. Bekdemir, Int. J. Quantum Chem. **111**, 3112 (2011).
12. B. Eren, and A. Ünal, Spectrochim. Acta, Part A **103**, 222 (2013).
13. H. Alyar, S. Alyar, A. Ünal, N. Özbek, E. Şahin, and N. Karacan, J. Mol. Struct. **1028**, 116 (2012).
14. B. Eren, S. Demir, H. Dal, and T. Hökelek, Acta Crystallogr. E **70**, 238 (2014).
15. A. D. Becke, J. Chem. Phys. **98**, 5648 (1993).
16. C. Lee, W. Yang, and R. G. Parr, Phys. Rev. B **37**, 785 (1988).
17. R. Ditchfield, W. J. Hehre, and J. A. Pople, J. Chem. Phys. **54**, 724 (1971).
18. M. J. Frisch, G. W. Trucks, H. B. Schlegel, G. E. Scuseria, M. A. Robb, J. R. Cheeseman, J. A. Montgomery, Jr., T. Vreven, K. N. Kudin, J. C. Burant, J. M. Millam, S. S. Iyengar, J. Tomasi, V. Barone, B. Mennucci, et al., *Gaussian 03, Revision E.01* (Gaussian, Inc., Wallingford, CT, 2004).
19. R. Dennington II, T. Keith, and J. Millam, *Gauss View, Version 4.1.2* (Semichem Inc., Shawnee Mission, KS, 2007).
20. M. P. Andersson and P. Uvdal, J. Phys. Chem. A **109**, 2937 (2005).
21. R. Ditchfield, J. Chem. Phys. **56**, 5688 (1972).
22. K. Wolinski, J. F. Hinton, and P. Pulay, J. Am. Chem. Soc. **112**, 8251 (1990).
23. E. Cancès, B. Mennucci, and J. Tomasi, J. Chem. Phys. **107**, 3032 (1997).
24. R. E. Stratmann, G. E. Scuseria, and M. J. Frisch, J. Chem. Phys. **109**, 8218 (1998).
25. M. E. Casida, C. Jamorski, K. C. Casida, and D. R. Salahub, J. Chem. Phys. **108**, 4439 (1998).
26. *National Committee for Clinical Laboratory Standards, Performance Standards for Antimicrobial Susceptibility Testing, 11th Informational Supplement,* M100-S11 (Nat. Committee Clin. Labor. Standard, Wayne, PA, USA, 2003).
27. I. Wiegand, K. Hilpert, and R. E. W. Hancock, Nat. Protoc. **3**, 163 (2008).
28. S. A. Sarker, L. Nahar, and Y. Kumarasamy, Methods **42**, 321 (2007).
29. A. L. Spek, Acta Crystallogr. D **65**, 148 (2009).
30. M. Karabacak, M. Cinar, and M. Kurt, J. Mol. Struct. **968**, 108 (2010).
31. V. Krishnakumar and R. Ramasamy, Spectrochim. Acta, Part A **62**, 570 (2005).
32. R. M. Silverstein, G. C. Bassler, and T. C. Morrill, *Spectrometric Identification of Organic Compounds* (Wiley, New York, 1981).
33. G. Varsanyi, *Assignments of Vibrational Spectra of 700 Benzene Derivatives* (Wiley, New York, 1974).
34. M. Karabacak, M. Cinar, and M. Kurt, J. Mol. Struct. **885**, 28 (2008).
35. D. Lin-Vien, N. B. Colthup, W. G. Fateley, and J. G. Grasselli, *The Handbook of Infrared and Raman Characteristic Frequencies of Organic Molecules* (Academic, Boston, 1991).
36. N. P. G. Roeges, *A Guide to the Complete Interpretation of Infrared Spectra of Organic Structures* (Wiley, New York, 1994).
37. R. M. Silverstein and F. X. Webster, *Spectrometric Identification of Organic Compounds* (Wiley, Asia, 2003).
38. K. Sarojini, H. Krishnan, C. C. Kanakam, and S. Muthu, Spectrochim. Acta, Part A **96**, 657 (2012).
39. B. T. Gowda, K. Jyothi, and J. D. D'Souza, Z. Naturforsch. A **57**, 9673 (2002).
40. K. L. Jayalakshmi and B. T. Gowda, Z. Naturforsch. A **59**, 491 (2004).
41. The Spectral Database for Organic Compounds SDBS. http://sdbs.db.aist.go.jp/sdbs/cgi-bin/direct_frame_top.cgi.
42. L. M. Jackman, and S. Stenhell, *Application of Nuclear Magnetic Resonance Spectroscopy in Organic Chemistry* (Pergamon Press, Oxford, 1969).
43. A. U. Rani, N. Sundaraganesan, M. Kurt, M. Cinar, and M. Karabacak, Spectrochim. Acta, Part A **75**, 1523 (2010).
44. V. Arjunan, R. Santhanam, T. Rani, H. Rosi, and S. Mohan, Spectrochim. Acta, Part A **104**, 182 (2013).
45. R. N. Jones, Chem. Rev. **32**, 1 (1943).
46. R. A. Friedel and M. Orchin, *UV Spectra of Aromatic Compounds* (Wiley, New York, 1951).
47. N. M. O'Boyle, A. L. Tenderholt, and K. M. Langner, J. Comput. Chem. **29**, 839 (2008).